

# A Laser-Based Coherent VUV Source and its Application to Highly Resolved Studies of the Fano Effect in HI

T. Huth-Fehre, A. Mank, M. Drescher, N. Böwering and U. Heinzmann

Fakultät für Physik, Universität Bielefeld, D-4800 Bielefeld, F.R.G.

Received July 16, 1989; accepted November 4, 1989

## Abstract

A highly resolving apparatus for molecular photoionization experiments based on resonantly enhanced sum-frequency mixing is discussed. The VUV source, based upon commercially available laser equipment, delivers more than  $10^{11}$  photons/second at a bandwidth of  $0.38 \text{ cm}^{-1}$  with linear or circular polarization. Results of photoelectron yield measurements obtained for the complete ( $n^* = 6$ ) Rydberg order of the autoionization resonances in the region of the spin-orbit split  $^2\Pi$  states of the  $\text{HI}^+$  ion are presented. In addition, measurements of the angle-integrated spin-polarization of the photoelectrons, ejected by circularly polarized radiation (Fano effect) are discussed.

## 1. Introduction

For a thorough understanding of the phenomena in molecular photoionization it is necessary to aim at resolving all underlying structure, including features due to vibration and rotation of the molecules. Typically, to obtain highly resolved molecular Rydberg spectra in photoabsorption studies, sophisticated vacuum spectrographs with resolving powers of  $R > 10^5$  in the vacuum ultraviolet (VUV) region are necessary [1].

In addition to photoabsorption studies it is desirable to analyze the emitted electrons in order to obtain a detailed characterization of the photoionization process by measuring the spectral dependence of the photoionization cross section, the energy and angular distributions as well as the spin-polarization vector of the photoelectrons. Such experiments were performed on free atoms, free molecules, adsorbates and solids using monochromatic synchrotron radiation as a light source [2]. Photoionization experiments on molecules, however, are restricted by the limited energy resolution of VUV monochromators. To combine high resolution studies with photoemission experiments, a narrowband light source with high spectral brightness is necessary. Using lasers one is not forced to trade bandwidth versus intensity: unfortunately, lasers are not readily available in the VUV. Nonlinear frequency mixing of pulsed dye laser radiation can be used for coherent VUV generation [3] in order to carry out single photon ionization experiments. A very efficient type of frequency upconversion is resonantly enhanced sum- and difference-frequency mixing [4]. This method is superior to simple frequency tripling since it combines resonant enhancement at the frequency of one laser with the tunability of a second laser, thus providing high spectral resolution ( $\Delta E < 1 \text{ cm}^{-1}$ ) together with high intensity, broad tunability, coherence and adjustable polarization. Resonantly enhanced sum frequency mixing in Hg [4] has already proved to be a powerful source of VUV radiation for photoelectron yield

measurements in the autoionization region between the thresholds corresponding to the spin-orbit split ground states of the  $\text{HI}^+$  ion [5]. Furthermore, the VUV source, based upon commercially available laser equipment, can be improved considerably in efficiency and long term stability.

The selection of the molecule HI was motivated in part by the *ab initio* calculation of the spin-orbit autoionization by Lefebvre-Brion and coworkers [6]. Using multichannel quantum defect theory (MQDT) they predicted the dynamical parameters of the photoionization process for the ( $n^* = 6$ )-member of the Rydberg series. Since the molecule is iso-electronic to the well-studied xenon atom, several photoionization and photoabsorption experiments were performed in the past pointing out similarities of the Rydberg structure. Eland and Berkowitz [7] and Dehmer and Chupka [8] have obtained spectra of the autoionization region of HI from photoionization mass spectrometry with a resolution of  $0.07 \text{ \AA}$  and  $0.15 \text{ \AA}$ , respectively. With a ten times higher resolution, measurements of the photoelectron yield [5] and of the angular distribution parameters  $\beta$  [9] were performed with the same source described here. Carlson et al. [10] have determined the cross section and the angular distribution parameter  $\beta$  applying photoelectron spectroscopy with synchrotron radiation at moderate resolution. In addition, a recent experiment using a laser-based light source [11] produced data for the photoelectron yield on HI, as well.

In this article we report the results of an experiment using sum-frequency mixing for single-photon ionization yield measurements in the VUV in the autoionization region between the  $\text{HI}^+ \ ^2\Pi$  ionic ground states. In addition, measurements of the angle-integrated spin-polarization of the photoelectrons ejected by circularly polarized radiation (Fano effect) are presented.

## 2. Experimental

The light source is based upon four-wave sum-frequency mixing in Hg vapor. A dye laser (Lambda Physics FL 3002E) produces radiation at  $\lambda = 560.4 \text{ nm}$ , which is frequency-doubled in a KDP crystal and tuned to the  $\text{Hg } 6s6d \ ^1D_2$  resonance at  $E = 71333.18 \text{ cm}^{-1}$  to enhance the efficiency of the conversion by a factor of  $\sim 500$  [4]. The third visible photon for the four-wave mixing, serving to tune the VUV-frequency, is produced by a second dye laser (Quanta Ray PDL 2). For pumping the two dye lasers two different schemes were tried out:

(1) Both dye lasers were pumped by the second harmonic (532 nm) of two different Nd:YAG lasers (Quanta

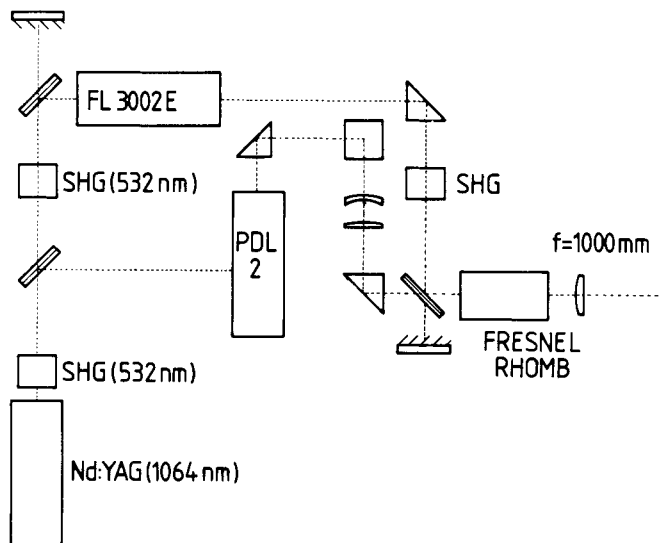


Fig. 1. Schematic diagram of the laser system. The outputs of both dye lasers (FL 3002E and PDL 2) are combined by a dichroic mirror (dm) before focussing into the mercury cell. (bs = beam splitter, bd = beam dump, dp = deflection prism).

Ray DCR2A and DCR22A) which were synchronized electronically.

(2) The second harmonic output of one of the YAG lasers (DCR2A) is separated from the residual fundamental beam by dichroic beamsplitters and used to pump the PDL with an energy of 150 mJ. In a second SHG stage the residual fundamental produces another 50 mJ of radiation with  $\lambda = 532$  nm. This is sufficient to obtain 20 mJ output from the FL laser which is operated with Rhodamine 6G dissolved in alkaline methanol.

This second scheme, shown in Fig. 1, was used to perform the experiments reported here. It produces a ten times higher VUV intensity and 50% less fluctuations than method 1 though the input power is smaller. The increase in intensity is due to the better beam profile (filled in beam option) of the DCR2A which is partially transferred to the dye laser outputs. The decrease of the fluctuations is caused by the elimination of the jitter in the electronics used for synchronization.

Both dye laser outputs are merged with a dichroic mirror, passed through a  $\lambda/2$  Fresnel rhomb and focussed into the mercury cell by means of a simple quartz lens ( $f = 100$  cm). The spatial overlap of the two foci is adjustable by prefocussing the visible laser beam in a Galilei-type telescope. 2 mJ of UV and 7 mJ of visible radiation finally reach the conversion cell.

For this cell the design reported in Ref. [4] was applied to produce a short but homogeneous zone of Hg vapor. Figure 2 shows the construction finally used. The long extensions between the windows and the main cell allow focussing ( $150 \text{ cm} > f > 30 \text{ cm}$ ) of the beams without damaging the windows. By making the extensions flexible the entire surface of the windows can be used to circumvent damaged spots. The lifetime of the windows was extended from one week to one year by freezing contaminations (water, hydrocarbons and mercury) on the walls of the extension tubes. Typically, the cell is operated at a Hg pressure of 9 mbar. To assure proper heat pipe operation, Neon (13 mbar) is added. Once a week the cell has to be pumped down to  $10^{-4}$  mbar due to small leaks at the O-ring sealed windows. Hence the cell can

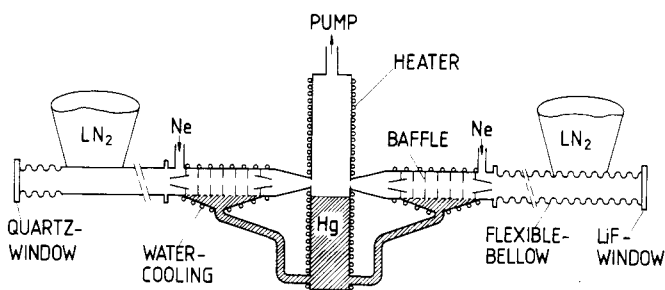


Fig. 2. Mercury conversion cell. The vapor zone for frequency conversion is located directly above the liquid in the central part and ends at the condensation baffles.

be operated for several days without maintenance. During a continuous run of 30 h the VUV intensity produced dropped less than 10% from the initial value.

Figure 3 shows the combination of the light source with the photoionization experiment, where HI molecules are ionized and the photoelectrons analyzed with respect to their intensity and spin-polarization. The molecular beam was produced by two different nozzles: a bent capillary plate forms a focussed beam with a rotational temperature close to room temperature and a pulsed valve (Lasertechnics LPV with  $300 \mu\text{m}$  orifice) cools the molecules considerably.

Performing multiphoton ionization via the  $c^3\Pi_1$ -state of HI [12] we measured the rotational temperature to be  $10 \text{ K} < T < 20 \text{ K}$ . Behind the target region the intensity of the VUV beam is monitored by an open photodiode. Assuming a quantum efficiency for the copper cathode of 4%,  $1 \times 10^{10}$  photons per pulse are detected at a repetition rate of 11 Hz.

The spectral resolution is measured to be better than  $0.7 \text{ cm}^{-1}$  ( $0.9 \times 10^{-3} \text{ nm}$ ) and can be calculated to be  $0.38 \text{ cm}^{-1}$  ( $5 \times 10^{-4} \text{ nm}$ ) by convoluting the energy uncertainties of the three photons used to produce the VUV. In order to avoid multiphoton processes and ionization at other frequencies also produced in the conversion cell [4] only the desired radiation is deflected into the target-region by means of a lithium fluoride (LiF) prism. Unfortunately, this prism exhibits a strong stress-induced birefringence which varies in strength locally. This stress seems to originate from the manufacturing process since a new second specimen showed the same behavior. The phase shift applied to a beam passing

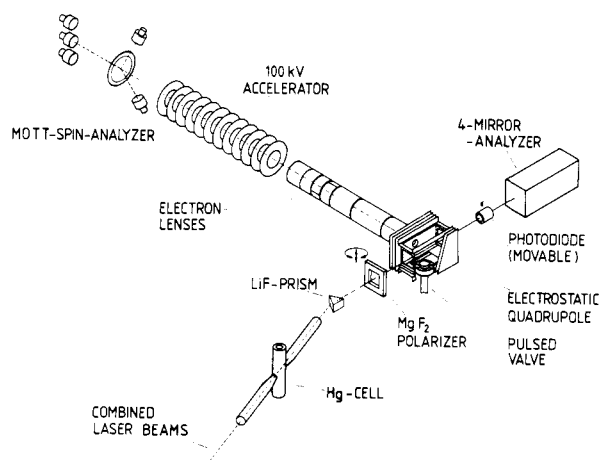


Fig. 3. Complete view of the experimental setup, showing the electron-optical system in detail.

through the prism, varies between  $\delta = 1.1 \pm 0.1^\circ$  at  $\lambda = 280$  nm and more than  $30^\circ$  at  $\lambda = 116$  nm. The axis of this birefringence is homogeneous through the whole crystal and parallel to the edges of the polished faces; hence exactly vertically or horizontally linearly polarized light passes the prism unaffected. A circular polarization of the VUV radiation beam (frequency upconverted circularly polarized visible laser beams) is partially depolarized by the birefringence.

For the measurement of the Fano effect the necessary circular polarization of the VUV is achieved by retarding linearly polarized radiation in a  $\text{MgF}_2$ -quarterwave plate of  $106 \mu\text{m}$  thickness. At  $86\,250 \text{ cm}^{-1}$  ( $115.94$  nm) this plate shows a transmission of 50% and the retardation depends strongly on the wavelength. By angle and temperature-tuning, the phaseshift can be adjusted to  $(n + \frac{1}{4})\lambda$  using a four-mirror reflection type analyzer (gold coated glass plates [13]) to check the polarization. Thus, a degree of circular polarization of  $(97 \pm 2.5\%)$  has been obtained in the photon energy range between  $85\,500$  and  $86\,500 \text{ cm}^{-1}$ .

The photoelectrons produced are collected by means of an electric field regardless of their kinetic energy and their direction of emission, and collimated. Subsequently, the photoelectrons are accelerated to an energy of 100 keV and scattered by a thin gold foil (Mott detector) for their spin-polarization analysis. A detailed description of this electron-optical system and the Mott detector is given in Ref. [14]. The scattered electrons as well as the beam in the forward direction are detected by surface barrier detectors and the charge produced during one laser pulse (3 ns) is registered by charge integrating preamplifiers. These signals are stored in sample-and-hold circuits, digitized and collected by a microcomputer. The procedure used for data processing is described in Ref. [5].

### 3. Results and discussion

The photoionization spectrum of HI between the  $^2\Pi_{3/2}$  ( $v = 0$ ) and  $^2\Pi_{1/2}$  ( $v = 0$ ) thresholds is dominated by resonances of the Rydberg series converging to the  $^2\Pi_{1/2}$  limit that are autoionizing via spin-orbit interaction in the  $^2\Pi_{3/2}$  ground state of the ion. In order to compare with the theoretical prediction [6], we will focus the discussion on the Rydberg order  $n^* = 6$ .

Our results for the photoelectron yield in this spectral region ( $85\,500$ – $86\,500 \text{ cm}^{-1}$ ) are shown in Fig. 4. The curve (a) was obtained using the warm molecular beam and the curve (b) shows our measurements on the molecules at temperatures of 10–20 K. The vertical lines at each data point represent the single statistical error. We digitized the 10 K spectrum of Hart and Hepburn [curve (c)] from the plot in Ref. [11] and converted the scale to wave numbers in order to compare it to our measurement. To indicate the uncertainties due to the digitalization we added error bars originating from this procedure to the data. The same processing was applied to obtain curve (d) from the theoretical data [6].

All four curves exhibit the same coarse features: At around  $85\,800 \text{ cm}^{-1}$  there are the strong and broad  $d\delta$  and  $d\pi$  resonances; sharper structures between  $85\,950 \text{ cm}^{-1}$  and  $86\,150 \text{ cm}^{-1}$  are related to the  $f\pi$  and  $f\sigma$  states of the Rydberg electron and a  $d\sigma$  resonance was calculated to lie at  $E = 86\,420 \text{ cm}^{-1}$ . The sharp resonances predicted in the

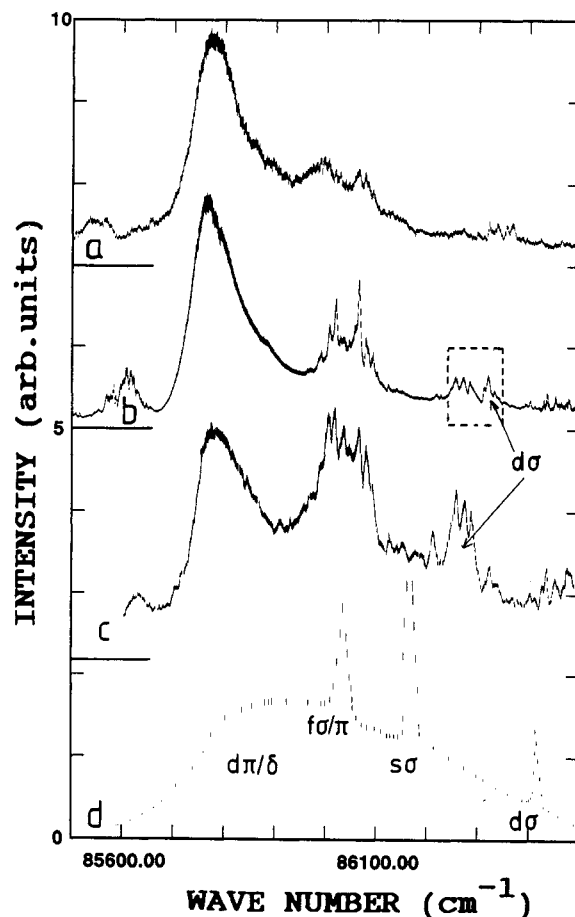


Fig. 4. Photoelectron yield spectra in comparison. (a) Our data (close to room temperature). (b) Our data at 10–20 K. (c) 10 K spectrum from Ref. [11]. (d) Theoretical curve from Ref. [6]. Curves (c) and (d) are taken from the publications, digitized and rescaled to wave numbers. For the error bars see text. A part of curve (b) (dashed box) is presented in detail in Fig. 5 on an enlarged scale.

calculation (neglecting rotational and vibrational effects) do not clearly appear in the warm spectrum due to the distribution of the total transition moment of a resonance onto the complete rotational branches. In the warm beam,  $J$  levels up to about  $J = 13$  are considerably populated with the maximum lying at  $J = 4$ . In addition to this, levels with higher  $J$  are distorted by a  $J$  dependent uncoupling of the angular moments  $L$  and  $S$  from the internuclear axis. Both effects are expected to be much weaker in a 10–20 K spectrum, where only levels with  $J = 0$  and  $J = 1$  are significantly populated. Thus, both cold spectra [curves (b) and (c)] show sharp structures. The calculation [curve (d)] shows much less structure than the experimental spectra due to the rotation neglected. The discrepancies in relative peak heights between the two cold measurements [curves (b) and (c)] seem to be related to different temperatures and problems with baseline normalization [15]. They are important, but lead to different conclusions in one case only:

The largest difference can be found in the spectral range between  $86\,200 \text{ cm}^{-1}$  and  $86\,400 \text{ cm}^{-1}$ , where the  $d\sigma$  resonance is expected to occur. In this region our first spin-polarization measurements were performed. They are shown in Fig. 5 together with an expansion from Fig. 4, curve b, as indicated by a box. In Ref. [11] the first three resonances were assigned to the  $d\sigma$  state, but the spin polarization clearly shows a sharp drop from a positive background to negative

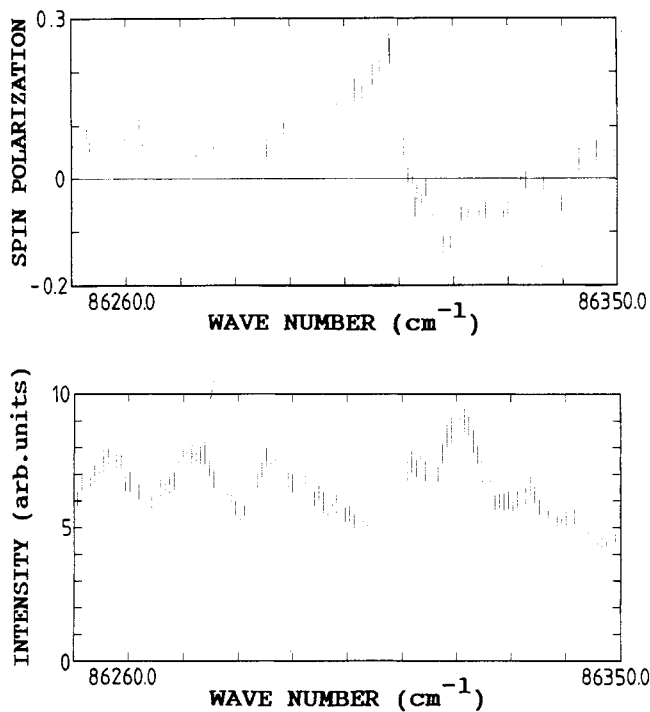


Fig. 5. Measured values of the photoelectron-spin-polarization normalized to an optical circular polarization of 100% (upper part) and the corresponding intensity yield. The vertical lines at each data point represent the experimental uncertainties.

values (theoretically predicted for  $\sigma$ -resonances) at a frequency ( $86310\text{ cm}^{-1}$ ) connected to the second set of peaks in the yield spectrum of Fig. 5. A proper assignment to rotational progressions is not possible for both interpretations; the interpretation in Ref. [11] requires the rotational constant  $B_0$  of the resonant level to be larger than  $6.8\text{ cm}^{-1}$  whereas the interpretation which is favored by the spin measurement, requires a strong perturbation of the  $Q_1$ -line since the second structure in the yield spectrum does not exhibit the correct rotational spacings. Measurements of the asymmetry parameter  $\beta$  [16] also support an interpretation involving a perturbation of the  $Q_1$ -line.

#### 4. Summary

The light source described could be improved considerably in efficiency and long-term stability. Since linearly as well as circularly polarized VUV radiation could be produced, it proved to be a reliable tool for detailed investigations of the photoelectron yield, the angular distribution parameter  $\beta$  [16] and measurements of the Fano effect.

#### Acknowledgement

We thank R. Wallenstein, G. Raseev and H. Lefebvre-Brion for valuable discussions. This work was supported by the Deutsche Forschungsgemeinschaft (SFB 216) and the European Commission.

#### References

- Ginter, M. L., Ginter, D. S. and Brown, C. M., *Appl. Opt.* **19**, 4015 (1980).
- Heinzmann, U., *Physica Scripta* **T17**, 77 (1986).
- Vidal, C. R., *Appl. Opt.* **19**, 3897 (1980).
- Hilbig, R. and Wallenstein, R., *IEEE J. Quantum Electr.* **EQ-19**, 1759 (1983).
- Huth, T., Mank, A., Böwering, N., Schönhense, G., Wallenstein, R. and Heinzmann, U., *Electronic and Atomic Collisions* (Edited by H. B. Gilbody, W. R. Newell, F. H. Read and A. C. H. Smith), p. 607. Elsevier Science Publishers (1988).
- Lefebvre-Brion, H., Giusti-Suzor, A. and Raseev, G., *J. Chem. Phys.* **83**, 1557 (1985).
- Eland, J. H. D. and Berkowitz, J., *J. Chem. Phys.* **67**, 5034 (1977).
- Dehmer, P. M. and Chupka, W. A., *Argonne Nat. Lab. Report ANL-78-65* (1978).
- Mank, A., Drescher, M., Huth-Fehre, T., Schönhense, G., Böwering, N. and Heinzmann, U., Submitted to *J. Phys.* **B22**, L487 (1989).
- Carlson, T. A., Gerard, P., Krause, M. O., von Wald, G., Taylor, J. W. and Grimm, F. A., *J. Chem. Phys.* **84**, 4755 (1986).
- Hart, D. J. and Hepburn, J. W., *Chem. Phys.* **129**, 51 (1989).
- Tilford, S. G., Ginter, M. L. and Bass, M., *J. Mol. Spec.* **34**, 327 (1970).
- Hunter, W. R., *Appl. Opt.* **17**, 1259 (1978).
- Möllenkamp, R. and Heinzmann, U., *J. Phys.* **E15**, 692 (1982).
- Hepburn, J. W., Private communication.
- Mank, A., Drescher, M., Huth-Fehre, T., Schönhense, G., Böwering, N. and Heinzmann, U., *J. of Electron Spectroscopy and Related Phenomena*, in print.